

PACS numbers: 31.10. + z, 31.15.ae, 31.15.A, 71.15 – m

## MATHEMATICAL SIMULATION OF GRAPHENE WITH MODIFIED C-C BOND LENGTH AND TRANSFER ENERGY

P.A. Alvi<sup>1\*</sup>, S.Z. Hashmi<sup>2</sup>, S. Dalela<sup>1</sup>, F. Rahman<sup>3</sup>

<sup>1</sup> Department of Physics, School of Physical Sciences,  
Banasthali University, Banasthali-304022, Rajasthan, India  
\* E-mail: [drpaalvi@gmail.com](mailto:drpaalvi@gmail.com)

<sup>2</sup> Department of Chemistry, Banasthali University,  
Banasthali-304022, Rajasthan, India

<sup>3</sup> Department of Physics, Aligarh Muslim University, Aligarh-202002, India

*In nanotechnology research, allotropes of carbon like Graphene, Fullerene (Buckyball) and Carbon nanotubes are widely used due to their remarkable properties. Electrical and mechanical properties of those allotropes vary with their molecular geometry. This paper is specially based on modeling and simulation of graphene in order to calculate energy band structure in  $k$  space with varying the C-C bond length and C-C transfer energy. Significant changes have been observed in the energy band structure of graphene due to variation in C-C bond length and C-C transfer energy. In particular, this paper focuses over the electronic structure of graphene within the frame work of tight binding approximation. It has been reported that conduction and valence states in graphene only meet at two points in  $k$ -space and that dispersion around these special points is conical.*

**Keywords:** GRAPHENE, TIGHT BINDING APPROXIMATION, ELECTRONIC STRUCTURE, TRANSFER ENERGY.

(Received 08 June 2011, in final form 29 September 2011  
published online 05 November 2011)

### 1. INTRODUCTION

Recently, graphene has been proved as a novel material in the new era of science and technology. Experimental results from transport measurements have shown that graphene has a remarkably high electron mobility at room temperature, with reported values in excess of  $15,000 \text{ cm}^2\text{V}^{-1}\text{s}^{-1}$  [1]. Additionally, the symmetry of the experimentally measured conductance indicates that the mobilities for holes and electrons should be nearly the same [2]. The mobility is nearly independent of temperature between 10 K and 100 K, which implies that the dominant scattering mechanism is defect scattering [3-5]. Due to its two-dimensional property, charge fractionalization is thought to occur in graphene. It may therefore be a suitable material for the construction of quantum computers using anyonic circuits [6].

Graphene's unique electronic properties produce an unexpectedly high opacity for an atomic monolayer, with a startlingly simple value: it absorbs  $\pi\alpha \approx 2.3 \%$  of white light, where  $\alpha$  is the fine-structure constant [7]. This is a consequence of the unusual low-energy electronic structure of monolayer graphene that features electron and hole conical bands meeting each other at

the Dirac point, which is qualitatively different from more common quadratic massive bands [8]. Recently it has been demonstrated that the band gap of graphene can be tuned from 0 to 0.25 eV (about 5 micrometer wavelength) by applying voltage to a dual-gate bilayer graphene field-effect transistor (FET) at room temperature [9]. The optical response of graphene nano ribbons has also been shown to be tunable into the terahertz regime by an applied magnetic field [10]. It has been shown that graphene/graphene oxide system exhibits electrochromic behavior, allowing tuning of both linear and ultrafast optical properties [11].

P. Shemella et al. [12] have studied the finite size effects on the electronic structure of graphene ribbons using first principles density functional techniques. The energy gap dependence for finite width and length has been computed for both armchair and zigzag ribbons. The results suggest, in addition to quantum confinement along the width of the ribbon, an additional finite size effect emerges along the length of ribbons only for metallic armchair ribbons. The finite size zigzag graphene ribbons, however, do not show any length dependence since the states near the Fermi energy are mostly derived from states located along the widths of ribbons. Such properties will be essential in designing future electronic devices. For example, for interconnect applications, where one needs metallic ribbons, zigzag ribbons will be of great interest. In contrast, for transistor applications, one would consider armchair ribbons with controlled band gaps. One possibility is to control the band gaps in finite size armchair ribbons is through functionalization.

Son et al. [13] calculated the energy band structure of graphene nano-ribbons and made estimations for the corresponding energy gap as a function of the width of nano-ribbons. They showed that the non-ribbons with both zig-zag and arm-chair boundaries would exhibit energy gap. Ohta et al. [14] have conducted a significant experimental study on the electronic band structure of a bi-layer graphene and observed that an electronic band gap at the Dirac point can be induced and controlled using an externally applied Coulomb potential. Pisani et al. [15] have studied the strong dependence of electronic structure of nano-ribbons on a magnetic field, and concluded the possible application of nano-ribbons of graphene in the controlled transport of spin and spintronics.

In the following sections of the paper, we have studied the energy band structure of the graphene with different geometry and modified C-C bond length and transfer energy between the C-C atoms. These parameters are, therefore, very important to control the energy band structure of the graphene, hence electrical and mechanical properties.

## 2. THEORETICAL AND SIMULATION DETAIL

Understanding the electronic structure of graphene is very important to describe the electronic states of a carbon nanotube because the cylindrical nanotube is formed from graphene – a honey-comb lattice of covalently bonded carbon atoms [16]. The graphene lattice has unique electronic properties. In Figure 1, the real space geometry of the graphene lattice is shown. Each unit cell has two carbon atoms, labeled A and B. The bonds between carbon atoms form a hexagonal lattice, with each A atom connected to three B atoms and vice versa. The bonds are directed along the vectors  $\vec{\rho}_1$ ,  $\vec{\rho}_2$ , and  $\vec{\rho}_3$ .

Each carbon atom has four valence electrons. Three of these electrons participate in the C-C sigma bonding. The fourth electron occupies a  $p_z$  orbital. The  $p_z$  states mix together forming delocalized electron states with a range of energies that includes the Fermi energy. These states are responsible for the electrical conductivity of graphene.

To proceed with a tight-binding calculation we build linear combinations of  $p_z$  orbitals that satisfy the symmetry of the graphene lattice. An electron wave function in a periodic lattice must satisfy the Bloch condition,

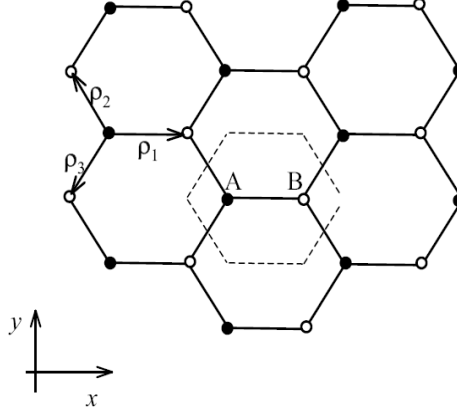


**Fig. 1** – Geometry of the graphene lattice. The unit cell, indicated by a dashed line, contains two carbon atoms labeled A (black) and B (white). The three bond vectors are labeled  $\vec{\rho}_1$ ,  $\vec{\rho}_2$ , and  $\vec{\rho}_3$ . The x axis is parallel to  $\vec{\rho}_1$

$$\psi_k(\vec{r}) = \exp(i\vec{k}\cdot\vec{r})u(\vec{r}), \quad (1)$$

where  $u(\vec{r})$  has the periodicity of the crystal lattice [17]. In the case of graphene, the function  $u(\vec{r})$  can be approximated using  $X(\vec{r})$ , the  $p_z$  atomic orbital of an isolated carbon atom. Positioning the function  $X(\vec{r})$  at every lattice site gives

$$\psi_k(\vec{r}) = \sum_A \exp(i\vec{k}\cdot\vec{R}_A)X(\vec{r} - \vec{R}_A) + \lambda \sum_B \exp(i\vec{k}\cdot\vec{R}_B)X(\vec{r} - \vec{R}_B), \quad (2)$$

where  $R_A$  and  $R_B$  are the positions of atoms A and B. The phase difference between two atoms in the same unit cell is  $\lambda \exp(i\vec{k}\cdot\vec{\rho}_1)$ , where  $\vec{\rho}_1$  is the bond vector connecting two atoms in the unit cell. Equation (2) satisfies the Bloch's theorem (1) i.e.  $\psi_k$  can be written in the form  $\exp(i\vec{k}\cdot\vec{r})u(\vec{r})$ .

Here first of all, we find out the eigen energies  $E_k$  of the wave states  $\psi_k$ . To approximate  $E_k = \langle \psi_k | H | \psi_k \rangle$  we start with an expression for  $\langle \psi_k | H | \psi_k \rangle$  that neglects the overlap integrals between the atoms A (each atom A is surrounded by atoms B);

$$E_k = E_o \pm \frac{1}{N} \int \left( \sum_A \exp(-i\vec{k}\cdot\vec{R}_A)X^*(\vec{r} - \vec{R}_A) \right) H \left( \lambda \sum_B \exp(-i\vec{k}\cdot\vec{R}_B)X(\vec{r} - \vec{R}_B) \right) d\vec{r} \quad (3)$$

where  $E_o$  is the energy of the bare  $p_z$  orbital,  $N$  is the number of carbon atoms in the lattice and  $H$  is the Hamiltonian describing the lattice. Equation (3) is further simplified by removing the remaining non-nearest neighbor terms;

$$E_k = E_o + \lambda \sum_i t_i \exp(-i\vec{k} \cdot \vec{\rho}_i), \quad (4)$$

with

$$t_i = \int X^*(\vec{r} - \vec{R}_A) H X(\vec{r} - \vec{R}_{B,i}) d\vec{r}, \quad (5)$$

where the index  $i = 1, 2$  or  $3$  refers to three B atoms neighboring each atom A.

The last step in determining  $E_k$  is finding the phase factor  $\lambda$ . From variational principles  $\lambda$  is a complex number of norm unity ( $|\lambda| = 1$ ) which makes equation (4) real valued [18].

Results obtained from [2], we have

$$E_k = E_o \pm \left| \sum_i t_i \exp(-i\vec{k} \cdot \vec{\rho}_i) \right|, \quad (6)$$

where  $\pm$  are associated with different values of  $\lambda$ .

There are two eigenvalues for every  $k$  in equation (6) due to the two possible values of  $\lambda$  at each point in  $k$  space. For example, at  $k = 0$  the high energy state has  $\lambda = 1$  while the low energy state has  $\lambda = -1$ . The two wavefunctions  $\psi_{k=0}^{\lambda=1}$  and  $\psi_{k=0}^{\lambda=-1}$  are shown in Figure 2. The phase of the wavefunction at each lattice site is designated by + or - signs.

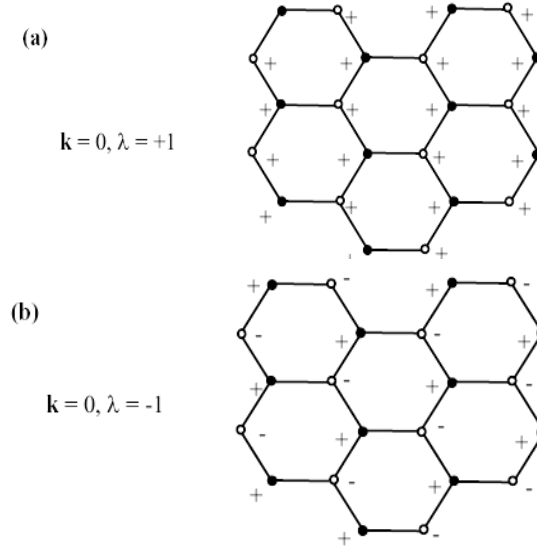


**Fig. 2** – Bonding and anti-bonding wavefunctions in graphene: when  $k = 0$ ,  $\lambda = 1$  all orbitals have the same phase and add constructively to form a bonding state (a), when  $k = 0$ ,  $\lambda = -1$  neighboring wavefunctions have opposite phase and an anti-bonding state is formed (b)

### 3. RESULTS AND DISCUSSION

The dispersion relation described by equation (6) is plotted for a graphene considered (of size  $12.78 \text{ \AA} \times 7.38 \text{ \AA}$  and zigzag in nature refer to figure 3) and shown in figure 4, 5 and 6. The modeled graphene under consideration (ref. Fig. 3) has its C-C bond length of  $1.42 \text{ \AA}$  and C-C transfer energy as  $3.0 \text{ eV}$  with the setting of overlap integral as  $0.129$ . In Figure 4 and 5, the energy of conduction and valence states for the zigzag graphene has been plotted separately as a function of wavevector  $k$ , while in Figure 6 the energy of conduction and valence states for the zigzag graphene has been plotted simultaneously in order to show its exact energy band structure. From Figure 6, we see that the conduction and valence bands meet at certain points in  $k$ -space. These special points, where conduction and valence states are degenerate, are called “K points”. Figure 7 shows a contour plot of the energy of valence band states. The circular contours around the K points reflect the conical shape of the dispersion relation near the K points. Electronic states near the Fermi level of graphene are located on dispersion cones. Therefore, the shape and position of these cones is critical for describing graphene (and nanotube) electronic properties. The two points  $K_1$  and  $K_2$  in Figure 7 are positioned at  $(k_x, K_y) = a^{-1}(0, \pm 4\pi/3)$ , where  $a$  is the magnitude of lattice vectors of graphene lattice. The slope of the cone is  $\sqrt{3}/2t_0a$ . The slope of the cones determines the Fermi velocity of graphene.

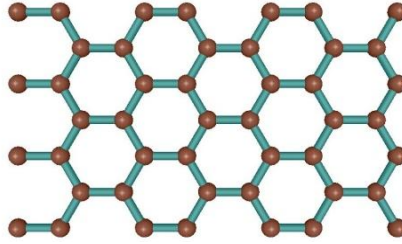


**Fig. 3** – Graphene view: zigzag in nature and having size  $12.78 \text{ \AA} \times 7.38 \text{ \AA}$

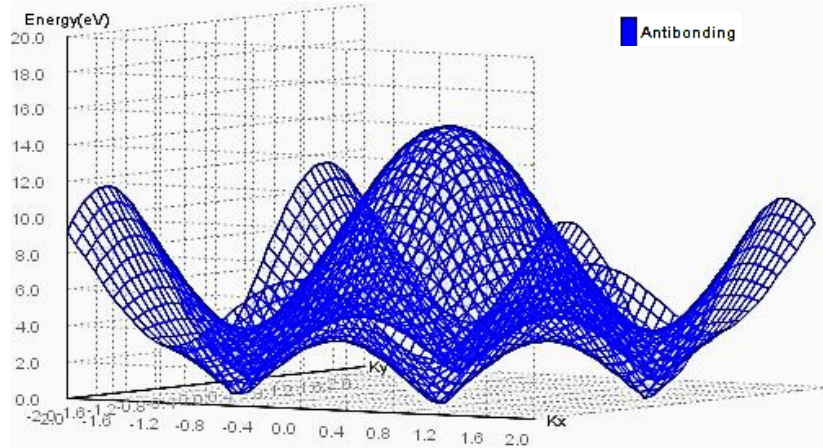


**Fig. 4** – The energy of conduction states in graphene plotted as a function of wavevector  $k$

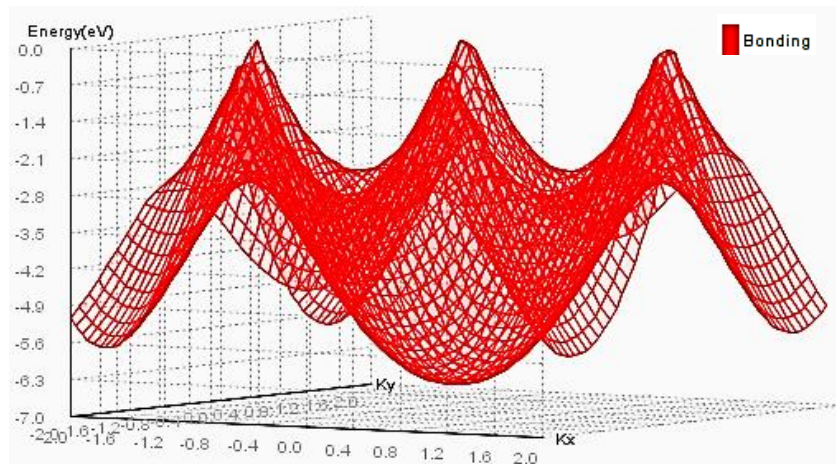


**Fig. 5** – The energy of valence states in graphene plotted as a function of wavevector  $k$

An important feature of Figure 6 is the vanishing energy difference between conduction and valence states at special points in  $k$ -space (the “K points”). The vanishing energy difference between conduction and valence states confirms metallic character of the zigzag graphene. By considering the symmetries of graphene we can gain a deeper understanding of this K point degeneracy. Symmetry arguments also show that there are only two inequivalent K points in graphene, and that this pair of points ( $K_1$  and  $K_2$ ) must satisfy the relationship  $K_1 = -K_2$ .

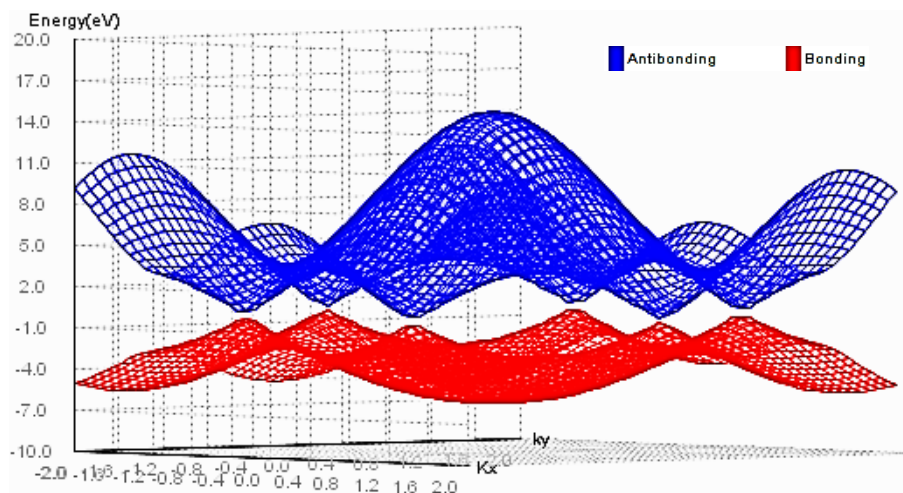


**Fig. 6** – The energy of conduction and valence states in graphene plotted as a function of wavevector  $k$ . Dispersion around these points is conical

K point degeneracy can be understood by considering states associated with the wave vector  $K_1 = (0, 4\pi/3)$ . With the help of this wave vector, a pair of wavefunctions (using two different values of  $\lambda$ ) can be constructed which demonstrate the physical basis for this degeneracy. The pair of

wavefunctions  $\Psi_{k_1}$  with  $\lambda = \exp(2\pi i/3)$  and  $\lambda = \exp(4\pi i/3)$  are shown in Figure 8. The phase of the wavefunction is indicated at each carbon atom. The wave functions map onto each other by a  $120^\circ$  rotation. Because the graphene lattice also has a  $120^\circ$  rotational symmetry, the two wavefunctions must be degenerate. Valence and conduction states with  $\mathbf{K}_1 = (0, 4\pi/3)$  are built from these degenerate  $\lambda = \exp(2\pi i/3)$  and  $\lambda = \exp(4\pi i/3)$  states. Therefore, valence and conduction states at the  $\mathbf{K}_1$  point are the

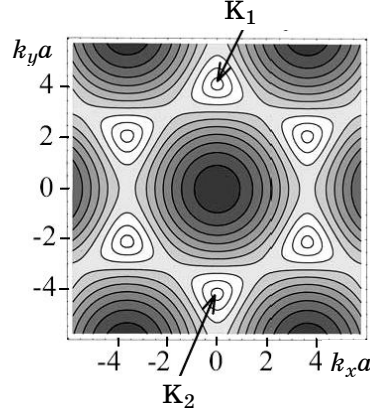


**Fig. 7** – A contour plot of the valence state energies. The hexagon formed by the six  $K$  points defines the graphene unit cell in  $k$ -space, beyond this unit cell the dispersion relation repeats itself. Arrows point to the two inequivalent  $K$  points,  $\mathbf{K}_1$  and  $\mathbf{K}_2$ .

degenerate. There are two further symmetries of graphene which are important for our analysis. The first is between  $\mathbf{k}$  and  $-\mathbf{k}$  states. If the conduction and valence states meet at  $\mathbf{K}_1$ , they must also meet at  $-\mathbf{K}_1$ . Therefore, the degeneracy we found at the  $\mathbf{K}_1$  point also occurs at  $\mathbf{K}_2 = -\mathbf{K}_1$ .

The impact of C-C bond length and C-C transfer energy on energy band structure can be understood with the help of dispersion relation. For the zigzag graphenes having C-C bond length of 1.00, 2.00 Å and C-C energy as 1.00, 2.00 eV while the overlap integral remaining unchanged, the change in energy band structures can be seen in figures 8 and 9 respectively. Although there is no change in the energy band gap between conduction band and valence band on changing the bond length and C-C transfer energy, but by carefully observing the scale of energy axis in the figures 8 and 9, it can be noted that the energy range of conduction states is increased due to which the curvature of conduction band is increased.

Hence, from Figure 8 and 9, it is clear that C-C bond length and C-C transfer energy have significant impact over the energy band structure of the graphene. Since, electrical and mechanical properties of graphene have already been reported to vary with their molecular geometry. The geometrical parameters of graphene are, therefore, very important to control the energy band structure of the graphene, hence electrical and mechanical properties. Graphene's modifiable chemistry, large surface area, atomic thickness and molecularly-gatable structure make antibody-functionalized graphene sheets excellent candidates for mammalian and microbial detection and diagnosis devices [19].

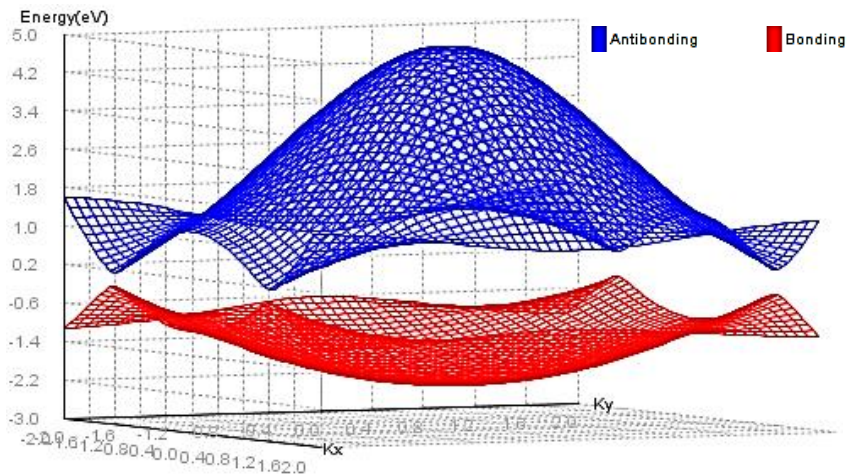


**Fig. 8** – The energy band structure for a graphene of C-C length 1.00 Å and C-C energy as 1.00 eV

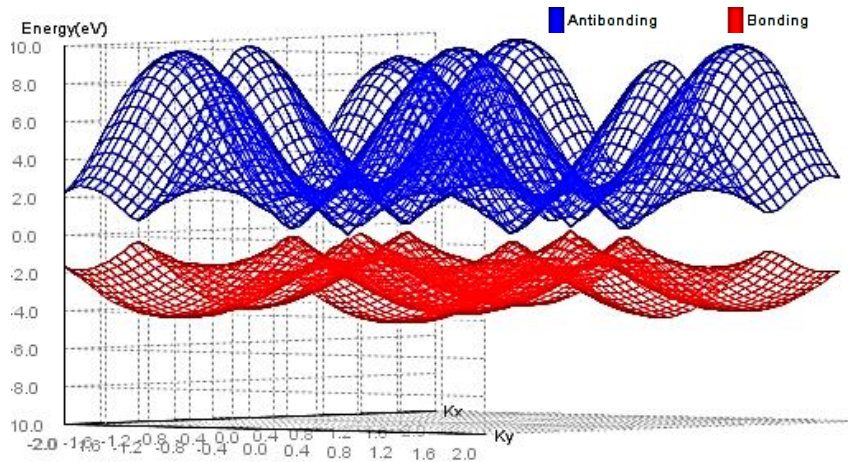


**Fig. 9** – The energy band structure for a graphene of C-C length 2.00 Å and C-C energy as 2.00 eV

#### 4. CONCLUSION

We have studied electronic structure of graphene within the frame work of tight binding approximation via modeling and simulation. Pronounced variations have been observed in the energy band structure of graphene due to variation in C-C bond length and C-C transfer energy. These parameters are, therefore, very important to control the energy band structure of the graphene, hence electrical and mechanical properties. Moreover, it has been observed that conduction and valence states in graphene only meet at two points in k-space and that dispersion around these special points is conical.

### ACKNOWLEDGEMENT

P.A. Alvi and S. Dalela are grateful to “Banasthali Center for Research and Education in Basic Sciences” under CURIE programme supported by the DST, Government of India, New-Delhi.

### REFERENCES

1. A.K. Geim, K.S. Novoselov, *Nat. Mater.* **6**, 183 (2007).
2. J.-C. Charlier, P.C. Eklund, J. Zhu, A.C. Ferrari, *Carbon Nanotubes: Advanced Topics in the Synthesis, Structure, Properties and Applications* (Berlin/Heidelberg: Springer-Verlag, 2008).
3. K.S. Novoselov, A.K. Geim, S.V. Morozov, D. Jiang, M.I. Katsnelson, I.V. Grigorieva, S.V. Dubonos, A.A. Firsov, *Nature* **438**, 197 (2005).
4. S.V. Morozov, K.S. Novoselov, M.I. Katsnelson, F. Schedin, D.C. Elias, J.A. Jaszczak, A.K. Geim, *Phys. Rev. Lett.* **100**, 016602 (2008).
5. J.H. Chen, C. Jang, S. Xiao, M. Ishigami, M.S. Fuhrer, *Nat. Nanotechnol.* **3**, 206 (2008).
6. J.K. Pachos, *Contemp. Phys.* **50**, 375 (2009).
7. A.B. Kuzmenko, E. van Heumen, F. Carbone, D. van der Marel, *Phys. Rev. Lett.* **100**, 117401(2008).
8. A.K. Geim, R.R. Nair, P. Blake, A.N. Grigorenko, K.S. Novoselov, T.J. Booth, T. Stauber, N.M.R. Peres, *Science* **320**, 1308 (2008).
9. Y. Zhang, T.-T. Tang, C. Girit, Z. Hao, M.C. Martin, A. Zettl, M.F. Crommie, Y.R. Shen, F. Wang, *Nature* **459**, 820 (2009).
10. Junfeng Liu, A.R. Wright, Chao Zhang, Zhongshui Ma, *Appl. Phys. Lett.* **93** 041106(2008).
11. U. Kurum, O. O. Ekiz, H. Gul Yaglioglu, A. Elmali, M. Urel, H. Guner, A.K. Mizrak, B. Ortac, A. Dana, *Appl. Phys. Lett.* **98**, 141103 (2011).
12. P. Shemella, Y. Zhang, M. Mailman, P.M. Ajayan, S.K. Nayak, *Appl. Phys. Lett.* **91**, 042101 (2007).
13. Y.W. Son, M.L. Cohen, S.G. Louie, *Phys. Rev. Lett.* **97**, 216803 (2006).
14. T. Ohta, A. Bostwick, T. Seyller, K. Horn, E. Rotenberg, *Science* **313**, 951 (2006).
15. L. Pisani, J.A. Chan, B. Montanari, N.M. Harrison, *Phys. Rev. B* **75**, 064418 (2007).
16. P.A. Alvi, K.M. Lal, M.J. Siddiqui, S. Alim, H. Naqvi, *Indian J. Pure Ap. Phy.* **43**, 899 (2005).
17. N.W. Ashcroft, N.D. Mermin, *Solid State Physics* (Orlando: Saunders College: 1976).
18. P.R. Wallace, *Phys. Rev.* **71**, 622 (1947).
19. N. Mohanty, B. Vikas, *Nano Lett.* **8**, 4469 (2008).